Electronic Supplementary Material (ESI) for Journal of Materials Chemistry C.

SUPPORTING INFORMATION

Ladder-Type Bithiophene Imide-Based Organic Semiconductors: Understanding charge transport mechanisms in Organic Field Effect Transistors

Alexandra Harbuzaru[‡*], Iratxe Arrechea-Marcos[‡], Alberto Scaccabarozzi[§], Yingfeng Wang[†], Xugang Guo[†], Mario Caironi[§*], J. Teodomiro López Navarrete[‡], M. Carmen Ruiz Delgado[‡], Rocio Ponce Ortiz[‡*]

[‡] Department of Physical Chemistry, University of Málaga, Campus de Teatinos s/n, Málaga 29071, Spain

[§] Center for Nano Science and Technology @ PoliMi, Istituto Italiano di Tecnologia, via Pascoli 70/3, 20133 Milano, Italy

[†] Department of Materials Science and Engineering, South University of Science and Technology (SUSTech), No. 1088, Xueyuan Road, Shenzhen, Guangdong 518055, China

Table of Contents

1. Spectroelectrochemical measurements of BTI2-BTI5.

The UV/Vis/NIR experiments were carried out on a Varian Cary 5000 UV-Vis-NIR spectrophotometer.

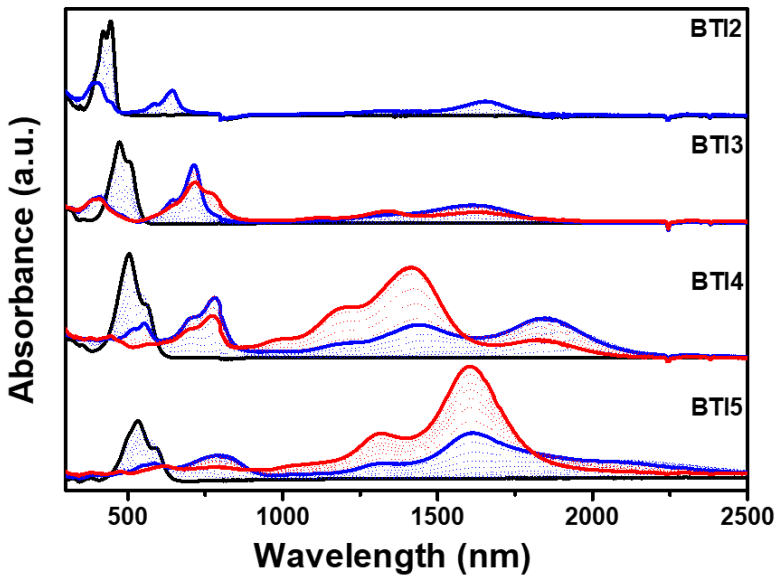

Figure S1. UV/Vis/NIR spectra changes upon electrochemical reduction of BTI2-BTI5 within an OTTLE cell in dichloromethane at room temperature in presence of 0.1 M (n-Hex)$_4$NPF$_6$ supporting electrolyte. The black, blue and red curves represent the neutral, radical anion and π-dimer dianion bands, respectively.

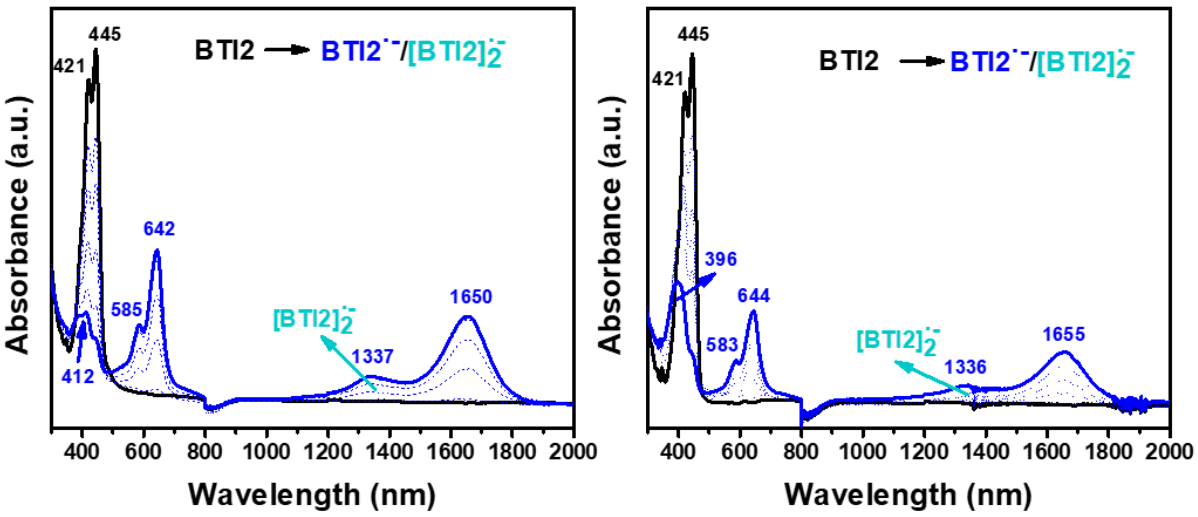

Figure S2. UV/Vis/NIR spectra changes upon electrochemical reduction of BTI2 within an OTTLE cell in dichloromethane at room temperature in presence of 0.1 M (n-Bu)$_4$NPF$_6$ (right) and (n-Hex)$_4$NPF$_6$ (left) supporting electrolytes. The black and blue curves represent the neutral and radical anion bands, respectively.

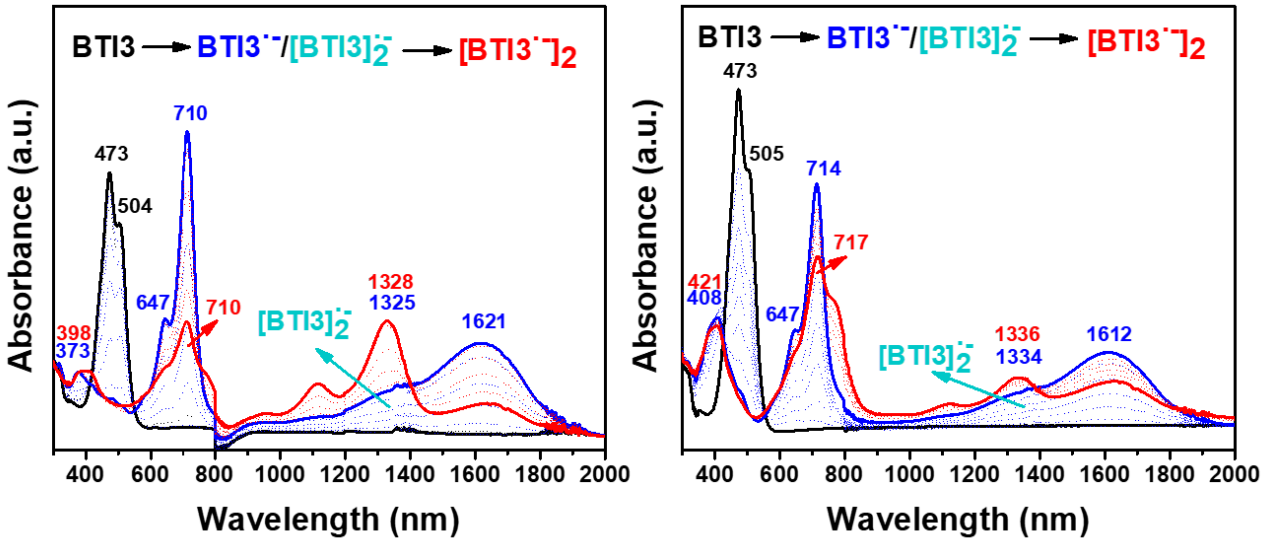

Figure S3. UV/Vis/NIR spectra changes upon electrochemical reduction of BTI3 within an OTTLE cell in dichloromethane at room temperature in presence of 0.1 M (n-Bu)$_4$NPF$_6$ (right) and (n-Hex)$_4$NPF$_6$ (left) supporting electrolytes. The black, blue and red curves represent the neutral, radical anion and π-dimer dianion bands, respectively.

2. DFT Calculations for BTI2-BTI5.

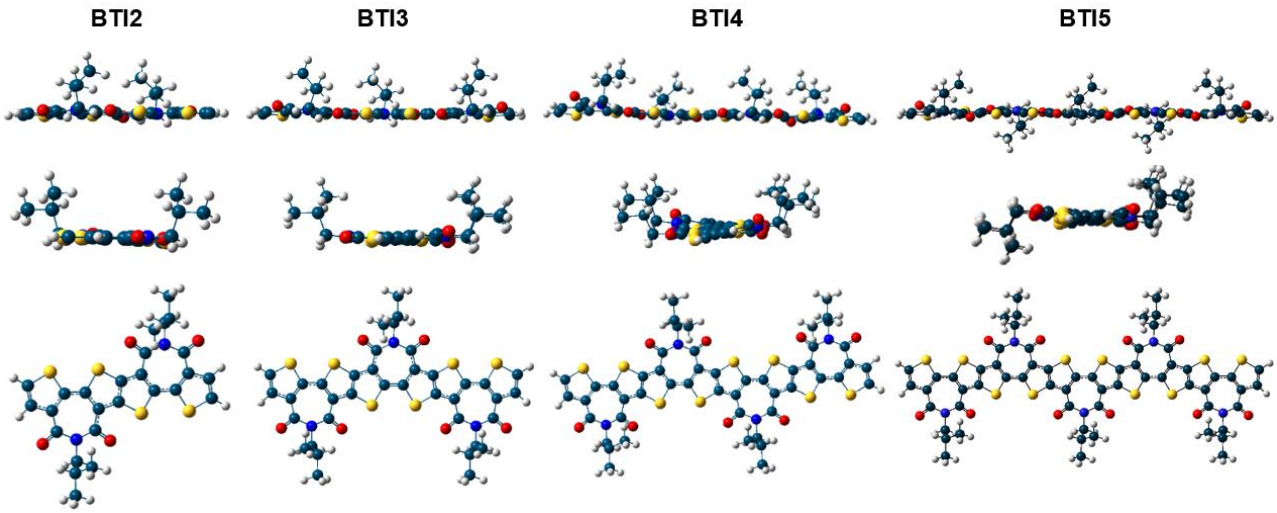

Figure S4. DFT optimized structures (frontal and lateral views) of BTI2-BTI5 monomers (LC-ωPBE-GD3BJ/6-31G**).

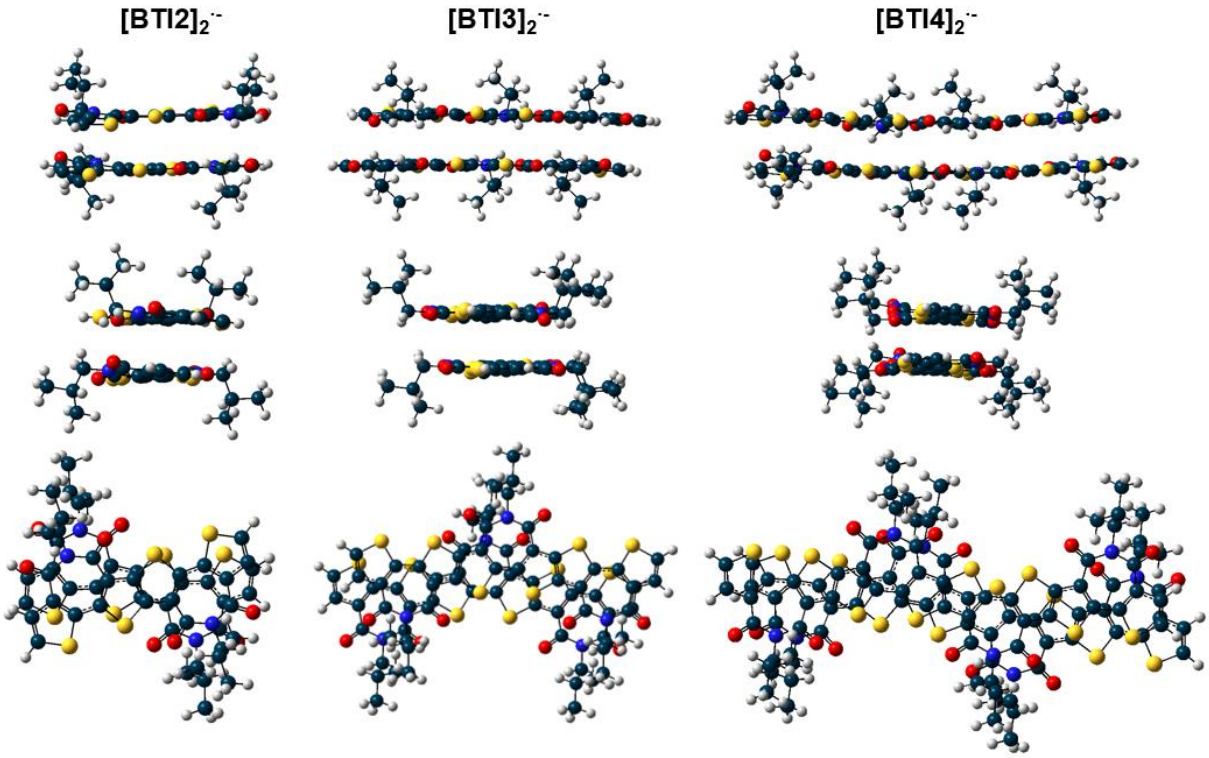

Figure S5. DFT optimized structures (frontal and lateral views) of BTI2, BTI3 and BTI4 parallel π-dimer radical anions (LC-ωPBE-GD3BJ/6-31G**).

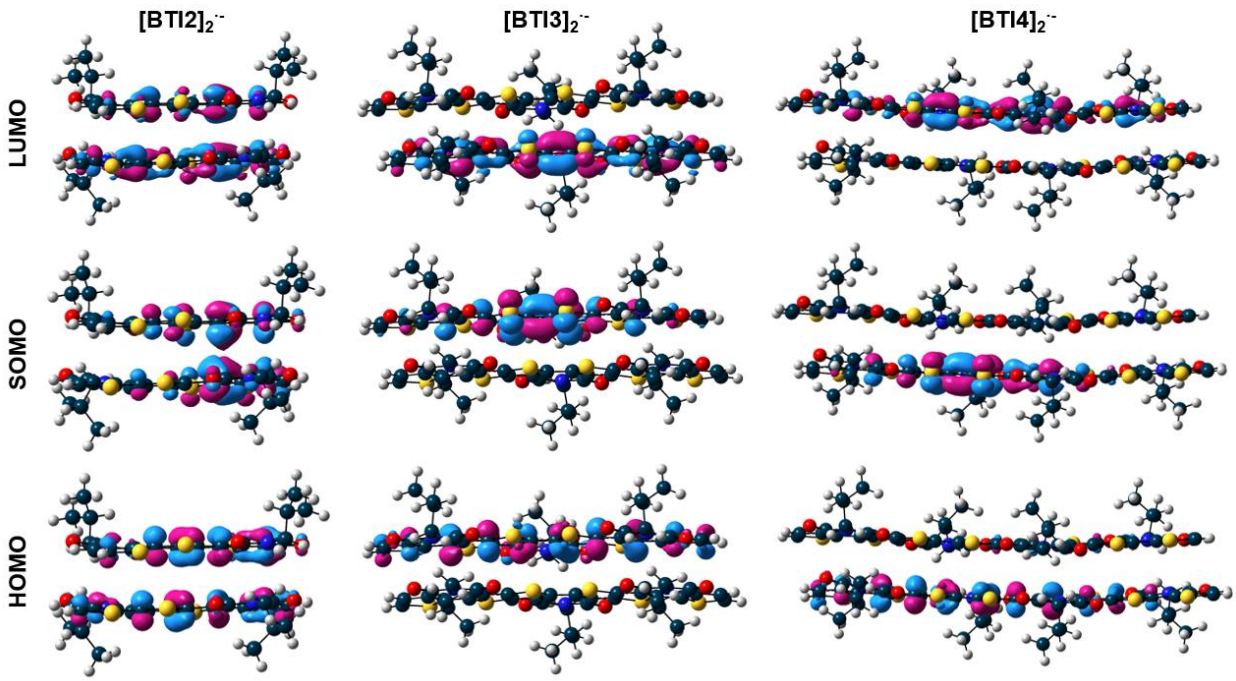

Figure S6. DFT optimized frontier molecular orbitals (HOMO, SOMO and LUMO) energy levels of BTI2-BTI4 π-dimer radical anions (LC-ωPBE-GD3BJ/6-31G**). Isovalue: 0.035.

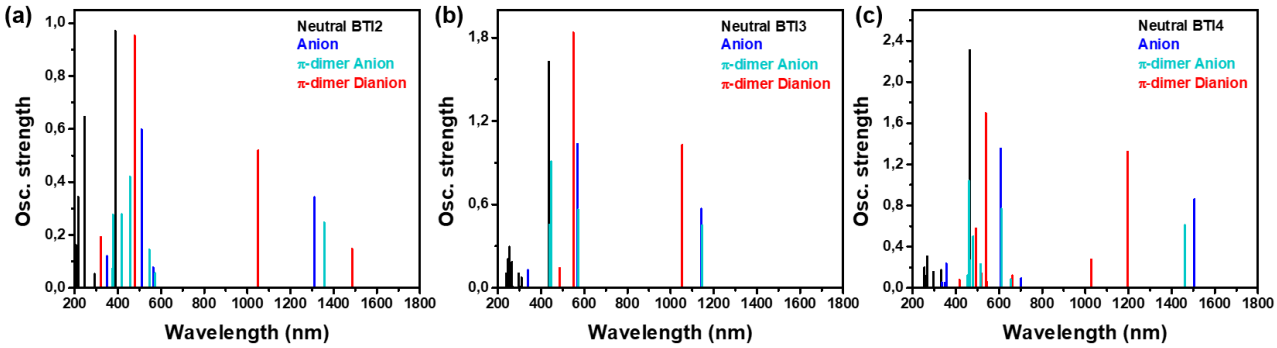

Figure S7. TD-DFT spectra calculated using the M06-2X functional over the previous M06-2X-GD3/6-31G**-optimized structures

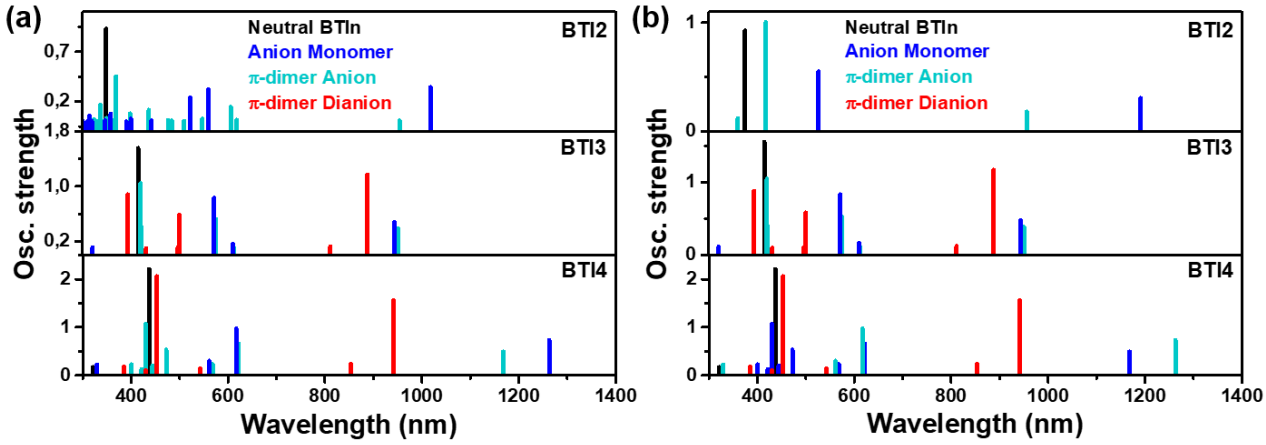

Figure S8. TD-DFT spectra calculated using the (a) LC-ωPBE and (b) wB97XD functionals over the previous LC-ωPBE-GD3BJ/6-31G**-optimized structures.

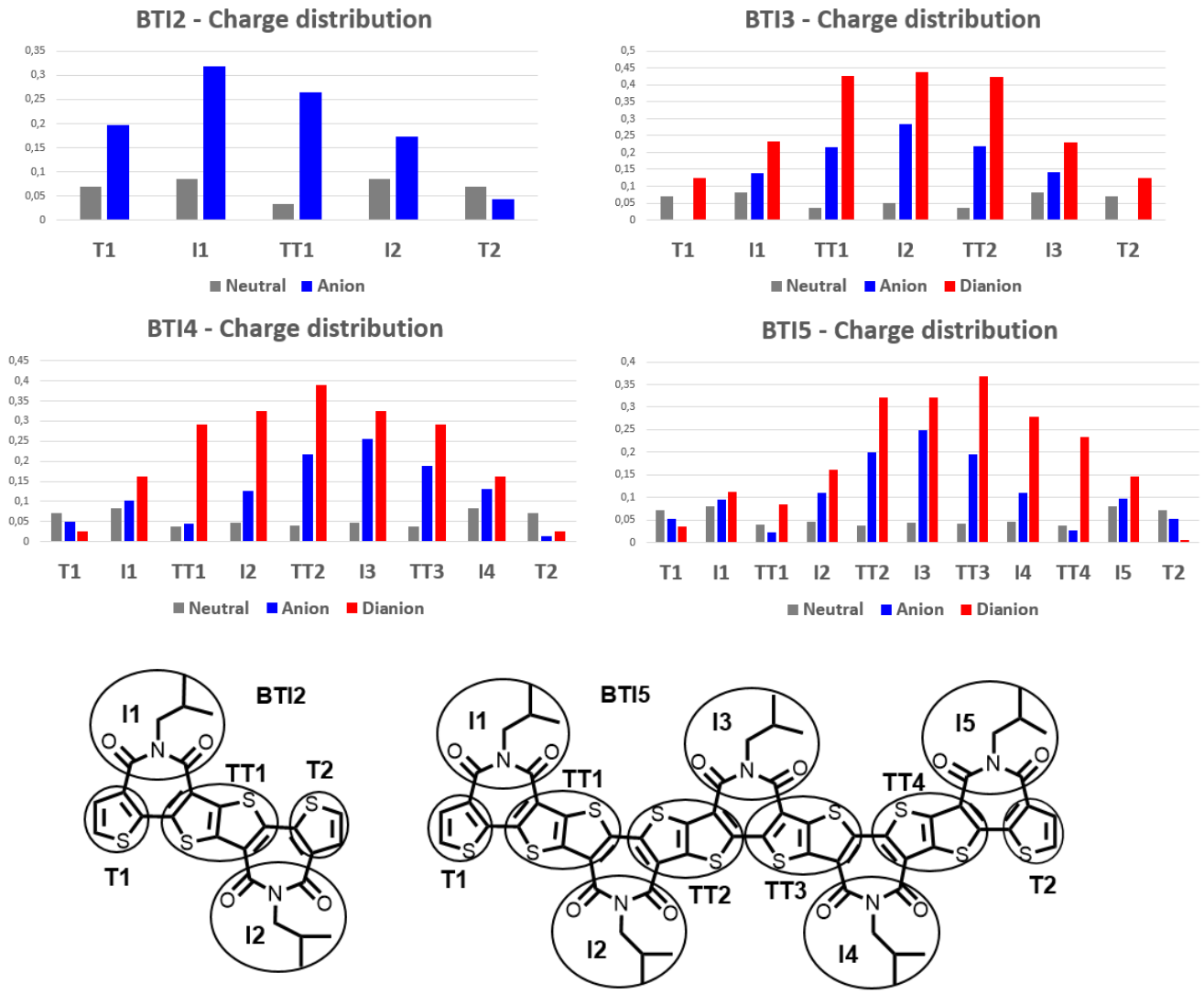

Figure S9. Selected Mülliken atomic charges on the molecular domains for the neutral, radical anion and dianion species of BTI2-BTI5 isolated monomers calculated at LC-ωPBE-GD3BJ/6-31G** level.

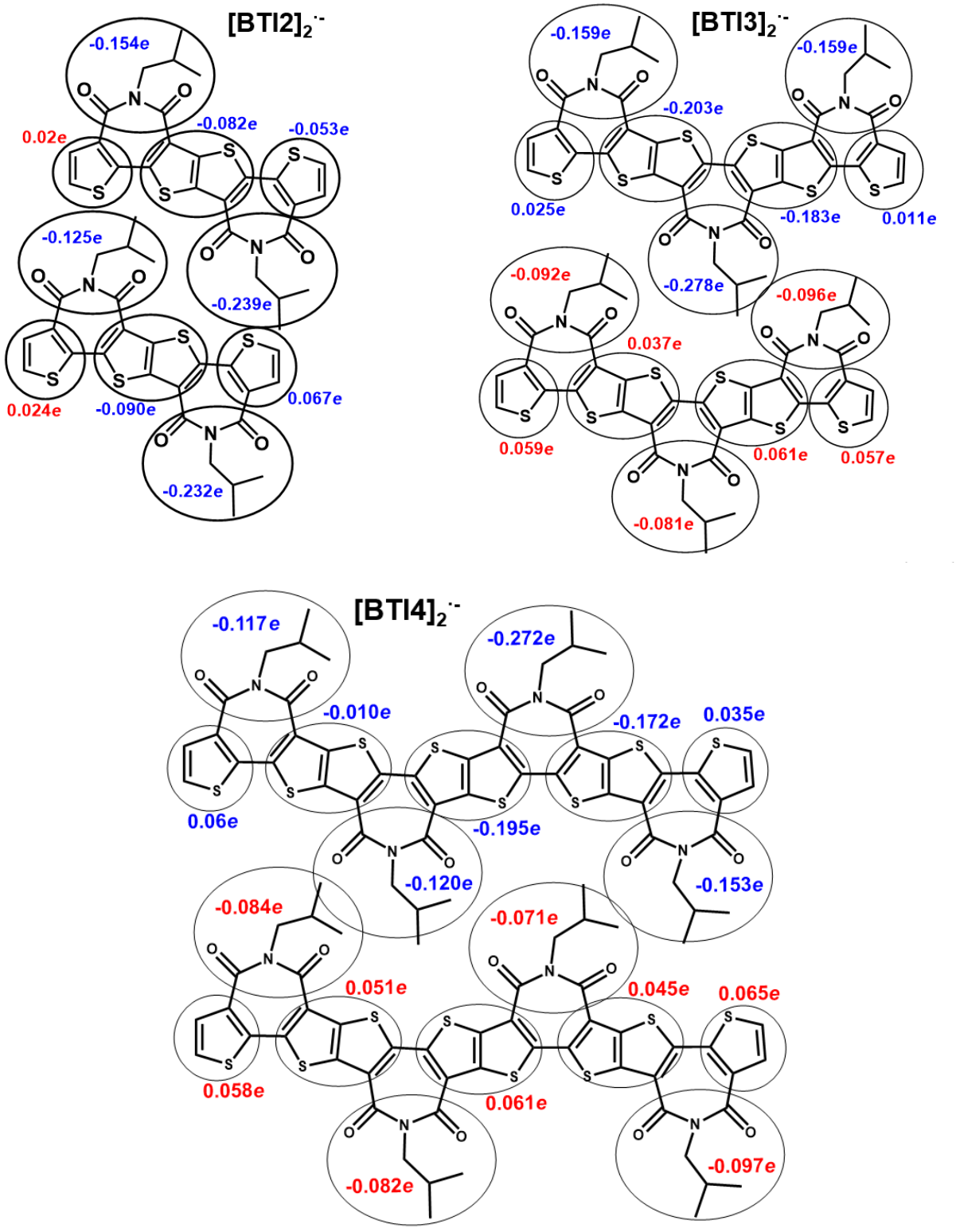

Figure S10. Selected Mülliken atomic charges on the molecular domains of BTI2-BTI4 π-dimer radical anions calculated at LC-ωPBE-GD3BJ/6-31G** level. The charge delocalization extension in the π-dimers is highlighted in blue.

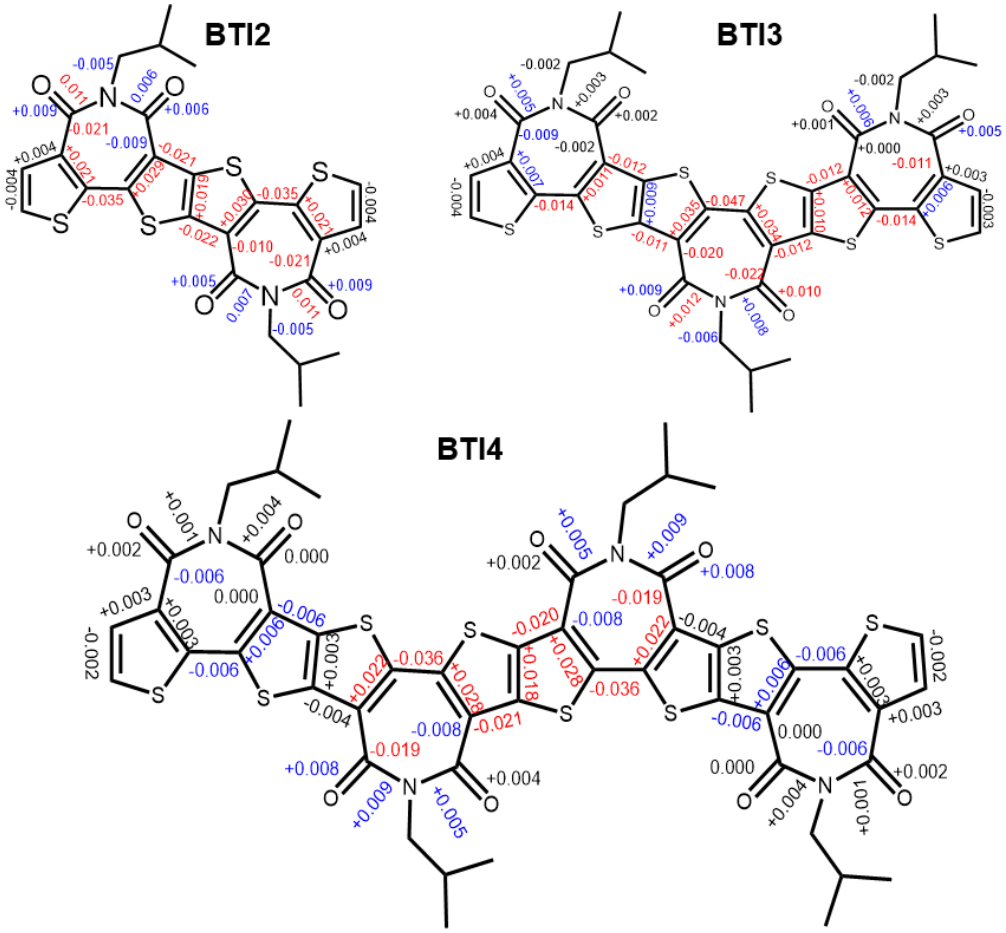

Figure S11. Selected bond length changes [Å] on the molecular domains of BTI2-BTI4 monomers when going from the neutral to the radical anion state calculated at LC-ωPBE-GD3BJ/6-31G** level. The bond length modifications (Δx) larger than 0.010 Å are highlighted in red and those highlighted in blue corresponds to 0.005 Å <Δx > 0.010 Å.

LC-ωPBE-GD3BJ/6-31G**

A) Binding Energy Calculation:

π-dimer radical anion, $[BTI2]_2^{\cdot-}$: *syn* disposition

1. Neutral monomer opt.: HF = - 3006.57887759
2. Radical anion monomer opt.: HF = - 3006.68408443

$\sum(HF)_{monomers\ opt.}$ = - 6013.26296202

3. π-dimer radical anion opt.: $HF_{\pi\text{-dimer opt}}$ = - 6013.31755851

E_{bind} (*syn* disposition) = $HF_{\pi\text{-dimer opt}}$ - $\sum(HF)_{monomers\ opt.}$ = -34.3 kcal/mol

π-dimer adical anion, $[BTI2]_2^{\cdot-}$: *anti* disposition

1. Neutral monomer opt.: HF = - 3006.57887759
2. Radical anion monomer opt.: HF = - 3006.68408443

$\sum(HF)_{monomers\ opt.}$ = - 6013.26296202

3. π-dimer radical anion opt.: $HF_{\pi\text{-dimer opt}}$ = - 6013.32020694

E_{bind} (*anti* disposition) = $HF_{\pi\text{-dimer opt}}$ - $\sum(HF)_{monomers\ opt.}$ = -35.9 kcal/mol

π-dimer dianion, $[BTI2^{\cdot-}]_2$: *syn* disposition

1. Radical anion monomer opt. x 2: HF = - 3006.68408443 x 2

$\sum(HF)_{monomers\ opt.}$ = - 6013.36816886

2. π-dimer dianion opt.: $HF_{\pi\text{-dimer opt}}$ = -6013.40256534

E_{bind} (*syn* disposition) = $HF_{\pi\text{-dimer opt}}$ - $\sum(HF)_{monomers\ opt.}$ = -21.6 kcal/mol

π-dimer dianion, $[BTI2^{\cdot-}]_2$: *anti* disposition

1. Radical anion monomer opt. x 2: HF = - 3006.68408443 x 2

$\sum(HF)_{monomers\ opt.}$ = - 6013.36816886

2. π-dimer dianion opt.: $HF_{\pi\text{-dimer opt}}$ = -6013.40138018

E_{bind} (*anti* disposition) = $HF_{\pi\text{-dimer opt}}$ - $\sum(HF)_{monomers\ opt.}$ = -20.8 kcal/mol

B) Interaction Energy Calculation:

π-dimer radical anion, $[BTI2]_2^{\cdot-}$: *syn* disposition

1. Neutral monomer sp: HF = -3006.57793307
2. Radical anion monomer sp: HF = -3006.68305285

$\sum(HF)_{monomers\ sp}$ = - 6013.26098592

3. π-dimer radical anion opt.: $HF_{\pi\text{-dimer opt}}$ = - 6013.31755851

E_{int} (*syn* disposition) = $HF_{\pi\text{-dimer opt}}$ - $\sum(HF)_{monomers\ sp}$ = - 35.5 kcal/mol

π-dimer radical anion, $[BTI2]_2^{\cdot-}$: *anti* disposition

1. Neutral monomer sp: HF = -3006.57736088
2. Radical anion monomer sp: HF = -3006.68275751

$\sum(HF)_{monomers\ sp}$ = - 6013.26011839

3. π-dimer radical anion opt.: $HF_{\pi\text{-dimer opt}}$ = - 6013.32020694

E_{int} (*anti* disposition) = $HF_{\pi\text{-dimer opt}}$ - $\sum(HF)_{monomers\ sp}$ = - 37.7 kcal/mol

π-dimer dianion, $[BTI2^{\cdot-}]_2$: *syn* disposition

1. Radical anion monomer sp: HF = - 3006.68328381
2. Radical anion monomer sp: HF = - 3006.68224394

$\sum(HF)_{monomers\ sp}$ = - 6013.36552775

3. π-dimer radical anion opt.: $HF_{\pi\text{-dimer opt}}$ = - 6013.40256534

E_{int} (*syn* disposition) = $H_{\pi\text{-dimer opt}}$ - $\sum(HF)_{monomers\ sp}$ = - 23.2 kcal/mol

π-dimer dianion, $[BTI2^{\cdot-}]_2$: *anti* disposition

1. Radical anion monomer sp: HF = - 3006.68245896
2. Radical anion monomer sp: HF = - 3006.68271960

$\sum(HF)_{monomers\ sp}$ = - 6013.36517856

3. π-dimer radical anion opt.: $HF_{\pi\text{-dimer opt}}$ = - 6013.40138018

E_{int} (*anti* disposition) = $HF_{\pi\text{-dimer opt}}$ - $\sum(HF)_{monomers\ sp}$ = - 22.7 kcal/mol

C) <u>Free Energy of formation Calculations (at 298 K):</u>

π-dimer radical anion, $[BTI2]_2^{\cdot-}$: *syn* disposition

4. Neutral monomer freq: Sum of electronic and thermal Free Energies = -3005.500159
5. Radical anion monomer freq: Sum of electronic and thermal Free Energies = -3005.610522

$\sum(E)_{monomers\ freq}$ = - 6011.110681

6. π-dimer radical anion freq.: Sum of electronic and thermal Free Energies = - 6011.133092

ΔG^0_f (*syn* disposition) = $E_{\pi\text{-dimer freq}}$ - $\sum(E)_{monomers\ freq}$= - 14.1 kcal/mol

π-dimer radical anion, $[BTI2]_2^{\cdot-}$: *anti* disposition

1. Neutral monomer freq: Sum of electronic and thermal Free Energies = -3005.500159
2. Radical anion monomer freq: Sum of electronic and thermal Free Energies = -3005.610522

$\sum(E)_{monomers\ freq}$ = - 6011.110681

3. π-dimer radical anion freq.: Sum of electronic and thermal Free Energies = - 6011.132166

$$\Delta G^0_f \text{ (}\textit{anti}\text{ disposition)} = E_{\pi\text{-dimer freq}} - \sum(E)_{\text{monomers freq}} = \mathbf{-13.5\ kcal/mol}$$

π-dimer dianion, $[BTI2^{\cdot-}]_2$: *syn* disposition

4. Radical anion monomer freq: Sum of electronic and thermal Free Energies = -3005.610522
5. Radical anion monomer freq: Sum of electronic and thermal Free Energies = -3005.610522

$$\sum(E)_{\text{monomers freq}} = -6011.221044$$

6. π-dimer radical anion freq.: Sum of electronic and thermal Free Energies = - 6011.214091

$$\Delta G^0_f \text{ (}\textit{syn}\text{ disposition)} = E_{\pi\text{-dimer freq}} - \sum(E)_{\text{monomers freq}} = \mathbf{4.4\ kcal/mol}$$

π-dimer dianion, $[BTI2^{\cdot-}]_2$: *anti* disposition

4. Radical anion monomer freq: Sum of electronic and thermal Free Energies = -3005.610522
5. Radical anion monomer freq: Sum of electronic and thermal Free Energies = -3005.610522

$$\sum(E)_{\text{monomers freq}} = -6011.221044$$

6. π-dimer radical anion freq.: Sum of electronic and thermal Free Energies = - 6011.213189

$$\Delta G^0_f \text{ (}\textit{anti}\text{ disposition)} = E_{\pi\text{-dimer freq}} - \sum(E)_{\text{monomers freq}} = \mathbf{4.9\ kcal/mol}$$

All the frequency calculations are carried out on the previously optimized systems at the same theoretical level. No imaginary frequencies were found.

3. Charge Modulation Spectroscopy (CMS).

The OTFT used for the CMS measurements, as a top-gate, bottom-contact architecture for optimized device performance.

Source-drain electrodes (3 nm Cr and 30 nm Au) were patterned on borosilicate glass substrates by photolithography. The substrates were subsequently cleaned by sonication in acetone, isopropanol followed by UV-ozone and oxygen plasma treatment. The semiconductor layers were spin-coated from 3 mg mL^{-1} anhydrous chloroform or tetrahydrofuran (THF) solutions and then were thermally annealed at 80°Cfor 30 min. Dielectric layers were spin coated from diluted CYTOP solutions (CTL-809M:CT-SOLV180 = 2:1 (v:v), Asahi Glass Co., Ltd.), then they were annealed at 80°C for 1 h. Finally, 50 nm Al was evaporated on top as the gate electrode. The devices were characterized with Keithley 4200 semiconductor characterization system. All device fabrication and characterization were carried out in N_2-filled glove box.

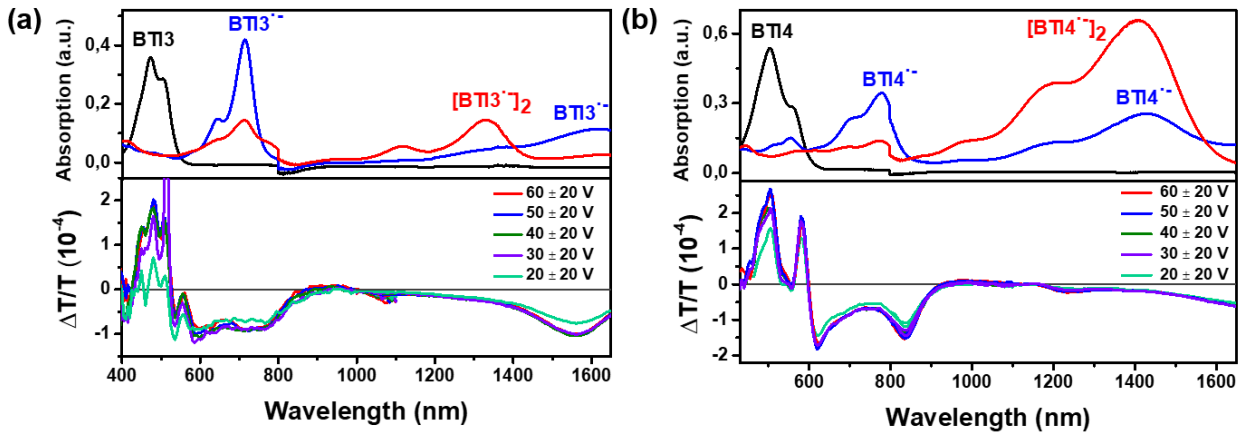

Figure S12. Top: UV/vis/NIR spectra changes at room temperature of a) BTI3 and (b) BTI4 within an OTTLE cell in dichloromethane containing 0.1 M $(n\text{-Bu})_4$ NPF_6 as supporting electrolytes. **Down:** Evolution of the CMS spectra of semitransparent OFETs with (a) BTI3 and (b) BTI4 semiconductors as the active material at T=300 K.

References

1. Riley, K. E., Pitoňák, M., Černý, J. & Hobza, P. On the Structure and Geometry of Biomolecular Binding Motifs (Hydrogen-Bonding, Stacking, X−H···π): WFT and DFT Calculations. *J. Chem. Theory Comput.* **6**, 66–80 (2010).
2. Grimme, S., Antony, J., Ehrlich, S. & Krieg, H. A consistent and accurate ab initio parametrization of density functional dispersion correction (DFT-D) for the 94 elements H-Pu. *J. Chem. Phys.* **132**, 154104 (2010).
3. Chai, J.-D. & Head-Gordon, M. Long-range corrected hybrid density functionals with damped atom–atom dispersion corrections. *Phys. Chem. Chem. Phys.* **10**, 6615–6620 (2008).
4. Vydrov, O. A. & Scuseria, G. E. Assessment of a long-range corrected hybrid functional. *J. Chem. Phys.* **125**, 234109 (2006).
5. Vydrov, O. A., Heyd, J., Krukau, A. V & Scuseria, G. E. Importance of short-range versus long-range Hartree-Fock exchange for the performance of hybrid density functionals. *J. Chem. Phys.* **125**, 74106 (2006).
6. Vydrov, O. A., Scuseria, G. E. & Perdew, J. P. Tests of functionals for systems with fractional electron number. *J. Chem. Phys.* **126**, 154109 (2007).
7. Grimme, S., Ehrlich, S. & Goerigk, L. Effect of the damping function in dispersion corrected density functional theory. *J. Comput. Chem.* **32**, 1456–1465 (2011).
8. Hehre, W. J., Ditchfield, R. & Pople, J. A. Self—Consistent Molecular Orbital Methods. XII. Further Extensions of Gaussian—Type Basis Sets for Use in Molecular Orbital Studies of Organic Molecules. *J. Chem. Phys.* **56**, 2257–2261 (1972).
9. Hariharan, P. C. & Pople, J. A. The influence of polarization functions on molecular orbital

hydrogenation energies. *Theor. Chim. Acta* **28**, 213–222 (1973).

10. M. J. Frisch, G. W. Trucks, H. B. Schlegel, G. E. Scuseria, M. A. Robb, J. R. Cheeseman, G. Scalmani, V. Barone, G. A. Petersson, H. Nakatsuji, X. Li, M. Caricato, A. V. Marenich, J. Bloino, B. G. Janesko, R. Gomperts, B. Mennucci, H. P. Hratchian, J. V., and D. J. F. Gaussian 16, Revision C.01,. (2016).

11. Tomasi, J., Mennucci, B. & Cammi, R. Quantum Mechanical Continuum Solvation Models. *Chem. Rev.* **105**, 2999–3094 (2005).

12. Improta, R., Barone, V., Scalmani, G. & Frisch, M. J. A state-specific polarizable continuum model time dependent density functional theory method for excited state calculations in solution. *J. Chem. Phys.* **125**, 54103 (2006).

13. Improta, R., Scalmani, G., Frisch, M. J. & Barone, V. Toward effective and reliable fluorescence energies in solution by a new state specific polarizable continuum model time dependent density functional theory approach. *J. Chem. Phys.* **127**, 74504 (2007).